Joint Pathology Center
Veterinary Pathology Services

WEDNESDAY SLIDE CONFERENCE 2026-2027

Conference #4 — 9 September 2026

CASE I:

Signalment:
3 month old male Han Wistar rat

History:
Low dose rat in a 6 week duration oral toxicity study. Rats were 6-7 weeks old at study start.

Gross Pathology:
At scheduled terminal necropsy, a 2.5 x 1.5 cm, pale cylindrical mass emanating from the outer medulla of one kidney and proceeding caudally was noted. The mass clearly compressed the adjacent renal parenchyma. No other masses were noted during the full necropsy of this rat.

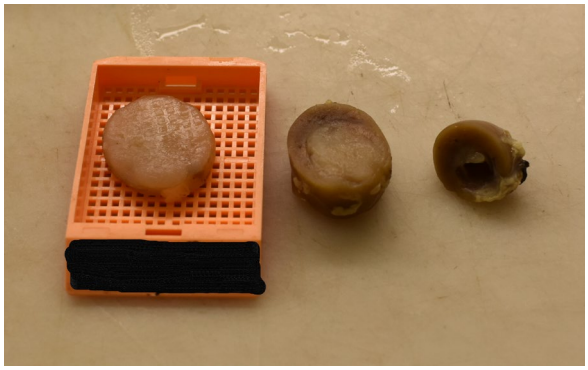

1-1. Kidney, rat (left to right): A transverse section of the mass which protruded from the caudal pole of the kidney; a transverse section showing the middle portion of the kidney with the pale, expansile mass visible in the medulla compressing the cortex; and the cranial pole of the kidney with two pale areas (*Photo courtesy of*: Drug Safety Research & Development, Pfizer Inc, www.pfizer.com)

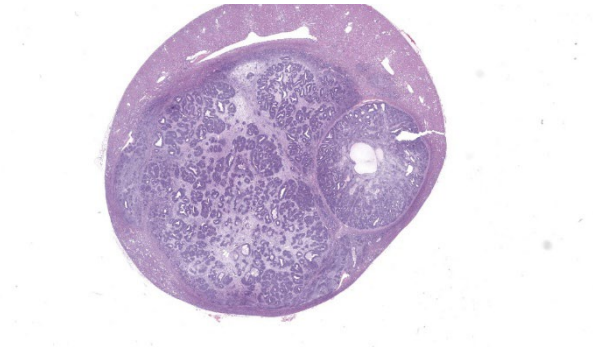

1-2. Kidney, rat: A large neoplasm compresses the medulla and pelvis and effaces approximately 80% of the renal parenchyma. Ectatic tubule-like structures are visible at this magnification. (HE, 10x).

Laboratory Results:
None provided.

Microscopic Description:
An expansile mass emanated from the corticomedullary junction of one kidney, obliterating the renal pelvis and nearly all of the medulla while compressing the remaining renal cortex. The mass was composed of biphasic islands of tubular structures (lined by darkly basophilic cuboidal to columnar epithelium when primitive, and lined with more eosinophilic, columnar epithelium when more mature) surrounded by darkly basophilic, crowded blastemal cells with occasional mitotic figures. These biphasic islands often touched and were either grouped into lobular structures separated from other portions of the mass by

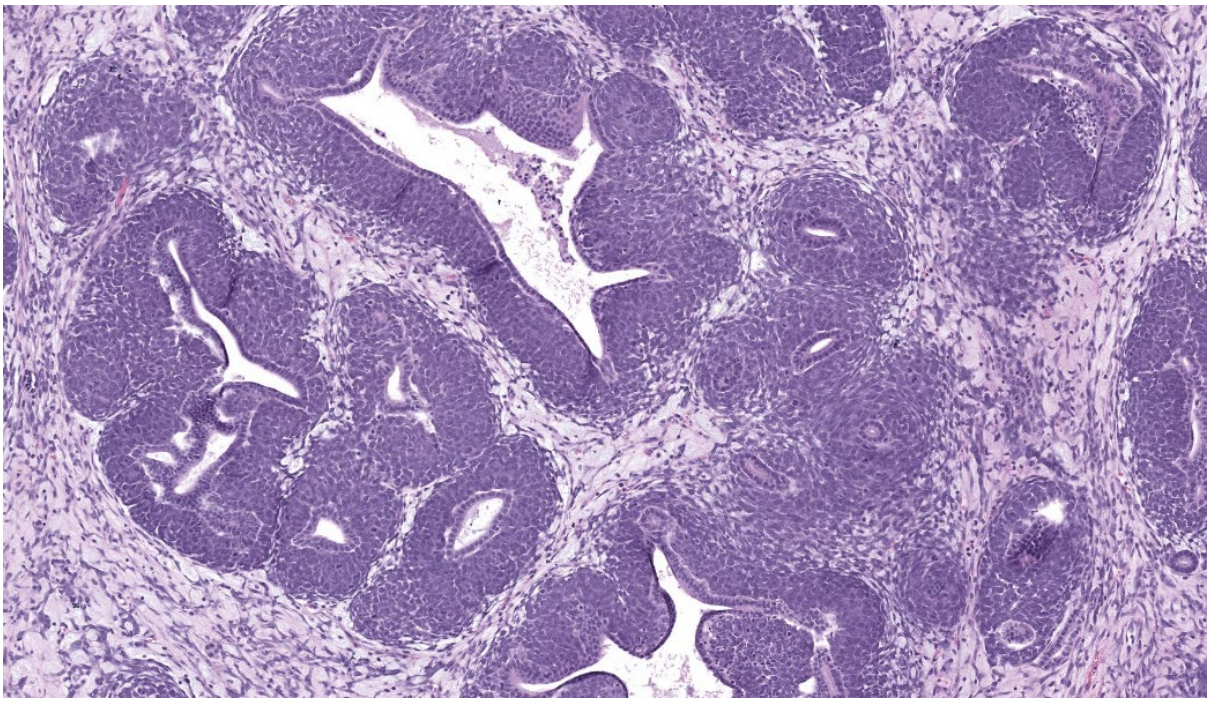

1-3. Kidney, rat: Irregularly shaped and ectatic tubules lined by columnar epithelium are surrounded by multiple layers of blastemal cells. These islands are surrounded and separated by elongate stromal cells on a myxomatous stroma. (HE, 101x).

denser connective tissue or were scattered amongst a more primitive connective tissue stroma. The islands were often crowded at the periphery of the lobules with the centers of the larger lobules having scattered islands, loose stroma, and in most slides, cystic structures. There was degeneration of some tubular epithelium in some islands with lumenal cellular debris and an amorphous eosinophilic substance. Near the outer edges of the main mass where it abutted with the remaining renal parenchyma were a few primitive glomerular structures (characterized by foci of small dark mononuclear cells). Local invasion of the mass into the remaining renal parenchyma was characterized by variously sized aggregates of blastemal cell associated with either loose or condensed stroma similar to that in the main mass. Due to the compression by the mass, mild tubular dilatation was present in the remaining renal parenchyma; a few dilated tubules in many slides contained cell debris and inflammatory cells or hyaline casts. There was minimal interstitial infiltrate in the renal parenchyma with little to no inflammatory response within the mass.

Contributor's Morphologic Diagnoses:
Nephroblastoma, unilateral (Incidental)
Tubular dilatation, multifocal, mild
Interstitial infiltrate, lymphocytic, minimal

Contributor's Comment:
The topographic origin (corticomedullary junction), contents (biphasic structures of blastemal cells surrounding primitive renal tubules and occasional primitive glomerular structures), and primitive loose connective tissue were all consistent with nephroblastoma.[2] Differential diagnoses were nephroblastemosis and renal mesenchymal tumor.[1,3] The extent of the mass alone was sufficient to exclude nephroblastemosis, which is a much smaller, typically interstitial, aggregate of primitive renal structures.[1] The remaining differential diagnosis, renal mesenchymal tumor,

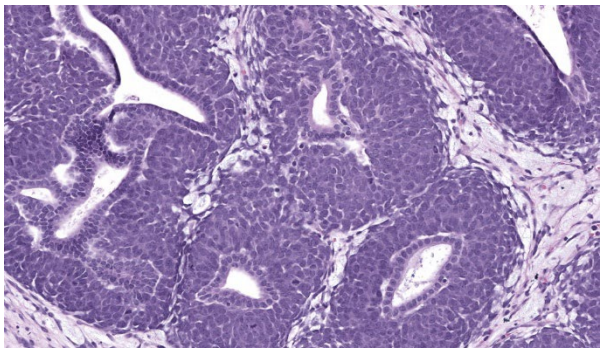

1-4. Kidney, rat: High magnification of neoplastic cells. In this field, mitotic figures are present in both the epithelial and blastemal populations. (HE, 381x).

is composed of several types of mesenchymally-derived structures, ranging from fibrous connective tissue to cartilage or bone and also contains entrapped but otherwise normal renal tubular elements.[2] None of these features were present in the mass evaluated.

Tumors in young adult rats can be an interpretive challenge in toxicity studies as they are uncommon and must be distinguished from an actual test article-related effect. Recent retrospectives and case reports have been vital in de-risking these rare spontaneous tumors from potential early carcinogenic signals.[3] The random placement of this particular rat into the low dose group was also helpful in the de-risking assessment in this case.

Contributing Institution:
Drug Safety Research & Development
Pfizer Inc.
www.Pfizer.com

JPC Diagnoses:
Kidney: Nephroblastoma

JPC Comment:
This week's moderator is our very own MAJ Sam Medlin, JPC Class of 2025 (that was a good year), Chief of the Necropsy Service at the Walter Reed Army Institute of Research, and a devotee of all things tumor. This week we covered some very interesting neoplasms from the stacks at the JPC, and found some surprising things in the process.

A nephroblastoma, also known as a Wilms tumor (WT), is an embryonal, mesodermal tumor with multiple lines of differentiation that is thought to arise from the primitive renal stem cells.[4] It is the most common renal tumor in childhood.[4] In human pediatric patients, it is associated with germline and/or somatic mutations of the WT1 gene, but other genes are thought to be involved as well.[3]

Histologically, WT presents with three distinct cell types: epithelial, stromal, and blastemal. All three elements are not required for diagnosis, but when all are present, the term "triphasic" is used. Like the renal mesenchymal tumor mentioned by the contributor, these tumors may also contain heterologous components, including smooth muscle, skeletal muscle, cartilage, and bone. All of the components of these tumors, including the heterologous components, have been shown to demonstrate similar genetic changes, indicating that all of these components are neoplastic.[6]

Nephroblastomas have been documented in a wide variety of domestic, laboratory, and exotic species, including dogs, cats, pigs, chickens, non-human primates, ruminants, camelids, rabbits, parakeets, and fish.[7,8,9,10] They

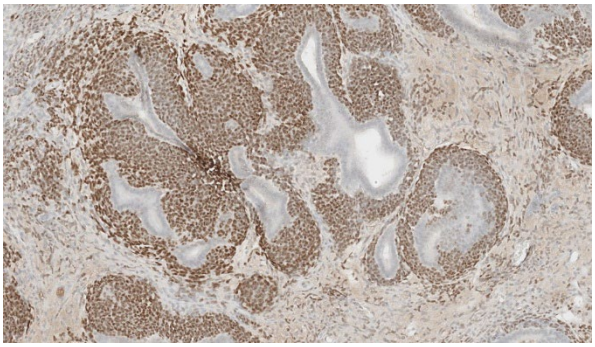

1-5. Kidney, rat: Blastemal cells demonstrate strong cytoplasmic immunoreactivity for Wilm's Tumor-1. (anti WT-1, 300x)

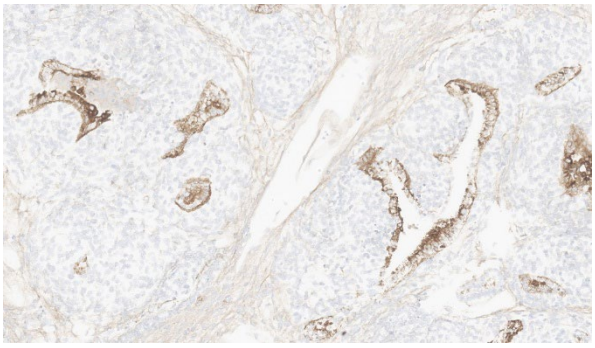

1-6. Kidney, rat: Epithelial cells demonstrate strong cytoplasmic immunoreactivity for cytokeratins. (anti AE1/AE3, 315x)

are considered the most common renal neoplasm in pigs, chickens, and fish.[7] In the dog, the spinal nephroblastoma (previously known by a wide range of names, including the early nomenclature of "thoracolumbar spinal tumor of young dogs") is an unusual manifestation of this tumor, which has previously been seen multiple times in the Wednesday Slide Conference (WSC 2013-2014 Conference 22, Case 3 and WSC 2019-2020, Conference 5, Case 4).[11] While the origin remains controversial, leading theories are that these tumors arise from either ectopic metanephric blastema or mesonephric rest tissue, either of which becomes entrapped between the dura mater and the spinal cord during embryogenesis.[12, 13]

In laboratory animals, nephroblastomas are most commonly reported in rats[14], and are less commonly seen in mice and non-human primates. In rats, nephroblastomas occur both experimentally and spontaneously.[14]

Experimentally, they have historically been induced by chemical administration of N-ethyl-N-nitrosourea or N-methyl-N-nitrosourea, both alkylating agents.[15] Spontaneously, they have been reported in Sprague-Dawley and F344 rats, with reports of metastases to the lymph nodes and lungs in these strains.[15,16]

References:

1. Kalaiselvan P, Mathur KY, Pande VV, Madheswaran R, Bhelonde JJ, Shelar PD, Udupa V, and Shingatgeri VM. Intralobar Nephroblastomatosis in a nine-week-old Wistar Rat. Toxicol Pathol 2009; 37:819-825.
2. Seely JC. Renal mesenchymal tumor vs nephroblastoma: revisited. J Toxicol Pathol 2004; 17:131-136.
3. Weber K. Differences in types and incidence of neoplasms in Wistar Han and Sprague-Dawley rats. Toxicol Pathol 2017; 45(1): 64-75.
4. Pritchard-Jones K. Malignant origin of the stromal component of Wilms' tumor. J Natl Cancer Inst. 1997; 89:1089–1091.
5. Beckwith J, Bruce NB, Bonadio K. Nephrogenic rests, nephroblastomatosis, and the pathogenesis of Wilms' tumor. *Pediatr Pathol*. 1990; 10:1-36
6. Zhuang Z, Merino MJ, Vortmeyer AO. Identical genetic changes in different histologic components of Wilms' tumors. J Natl Cancer Inst. 1997; 89:1148-52.
7. Meuten DJ, Meuten TLK. Tumors of the urinary system. In: Meuten DJ, ed. *Tumors in Domestic Animals.* 5th ed. Ames, Iowa: Iowa State Press; 2017:646-649.
8. Delaney MA, Treuting PM, Rothenburger JL. Lagamorpha. In: Terio KA, McAloose D, St. Leger J, eds. *Pathology of Wildlife and Zoo Animals.* San Diego, CA: Elsevier. 2018; 486.
9. Frasca Jr S, Wolf JC, Kinsel MJ, Camus AC, Lombardini ED. Osteichthyes. In: Terio KA, McAloose D, St. Leger J,

eds. *Pathology of Wildlife and Zoo Animals.* San Diego, CA: Elsevier. 2018; 961.

10. Reavill DR, Dorrenstein G. Psittacines, Coliiformes, Musophagiformes, Cuculiformes. In: Terio KA, McAloose D, St. Leger J, eds. *Pathology of Wildlife 11. and Zoo Animals.* San Diego, CA: Elsevier. 2018; 784.
11. Brewer DM, Cerda-Gonzalez S, Dewey CW, Diep AN, Van Horne K, McDonough SP. Spinal cord nephroblastoma in dogs: 11 cases (1985-2007). J Am Vet Med Assoc. 2011; 238(5):618-24.
12. Gasser, AM., Bush, WW., Smith, S., Walton, R. Extradural spinal, bone marrow, and renal nephroblastoma. J Am Anim Hosp Assoc. 2003; 39: 80-85.
13. Petit A, Rubio A, Durand C, Piolat C, Perret C, Pagnier A, Plantaz D, Sartelet H. A Wilms' Tumor with Spinal Cord Compression: An Extrarenal Origin? Case Rep Pediatr. 2018 Sep 3;2018:1709271.
14. Chandra M, Carlton WW. Incidence, histopathologic and electron microscopic features of spontaneous nephroblastomas in rats. *Toxico Lett.* 1992; 62: 179-190.
15. Yoshizawa K, Kinoshita Y, Emoto Y. N-Methyl-N-nitrosourea-induced Renal Tumors in Rats: Immunohistochemical Comparison to Human Wilms Tumors. *J Toxicol Pathol.* 2014; 26:141-148.
16. Tanaka, N., Takeshi, I., Jyoji, Y. Spontaneous nephroblastoma with striated muscle differentiation in an F344 rat. *J Toxicol Pathol.* 2017; 30:231-234.

CASE II:

Signalment:
12 year-old, female, Bouvier des Flandres dog (*Canis lupis familiaris*)

History:
Straining to defecate for several days. Rectal palpation revealed a 1.5 cm nodule just inside the anus. The mass was surgically excised and submitted for histopathologic examination.

Gross Pathology:
Received a 1.8 x 1.5 x 0.8 cm brown tissue. The surgical border could not be identified at the time of sectioning.

Laboratory Results:
In formalin-fixed, paraffin- embedded sections of the rectal mass the tumor cells exhibited positive pyronophilia with methyl green pyronin. The deposits of amyloid stained with Congo red and exhibited some apple-green birefringence under polarized light. The birefringence was resistant to pretreatment with potassium permanganate supporting immunoglobulin-derived amyloid (primary) composed of lambda light chains. The tumor cells were immunohistochemically positive for lambda light chains.

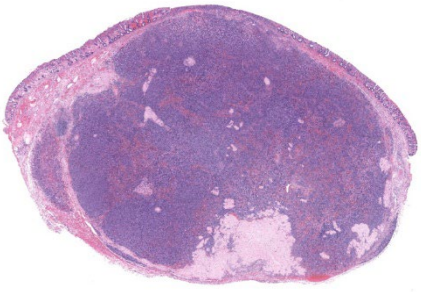

2-1. Colon, dog: There is a well-demarcated round cell neoplasm infiltrating and expanding the colonic wall affecting the mucosa, submucosa, and smooth muscle. There are large islands of amyloid scattered through the tumor, with a predominance in deeper areas of the neoplasm. (HE, 16x)

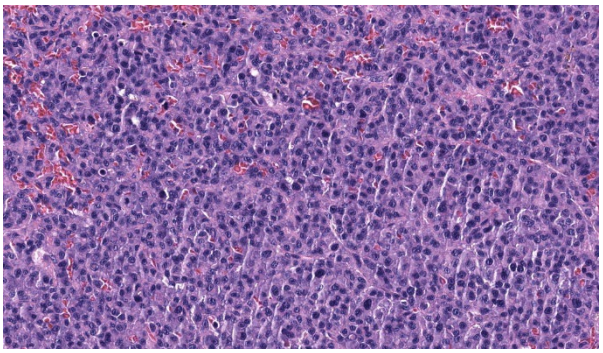

2-2. Colon, dog: Neoplastic round cells are arranged in nests and packets. (HE, 572x)

Microscopic Description:
In the submucosa there is a poorly demarcated, compressive, unencapsulated mass that comprises packets, supported by thin strands of fibrovascular connective tissue, and sheets of round cells with distinct cell borders and a moderate to high nuclear to cytoplasmic ratio. Tumor cells are close to or at all of the circumferential surgical borders. The nucleus is eccentric, round to oval to indented to bizarre (lobulated forms seen) with a finely to coarsely stippled chromatin pattern. Occasional cells possess one to two, large, round nucleoli. The cytoplasm is scant to moderate and blue. Many cells have a paranuclear clear zone and some cells possess a few large, pink globules. Some cells appear to contain a coarsely granular, golden brown pigment (hemosiderin?). Anisokaryosis is moderate. Multinucleate forms (up to 3 nuclei seen) are rare. Karyomegaly is frequent. Mitoses are seen (0-2 per 40X objective fields). There are several foci of hemorrhage accompanied by a few hemosiderophages in the mass.There are extracellular collections of a pale pink, homogeneous material that is interpreted to be amyloid. The mucosa is multifocally ulcerated and there is a moderate infiltrate of neutrophils, small lymphocytes and plasma cells in the lamina propria. Hemorrhage is present in the lamina propria and submucosa.

Contributor's Morphologic Diagnoses:
Rectal mass: Colonic extramedullary plasmacytoma (EMP) with intralesional primary amyloid deposition

Contributor's Comment:
The incidence of rectal and colonic EMPs has been reported to be 4.0% of all canine EMPs[2]. Other reported locations include cutaneous sites (86%; mostly on the skin of the limbs, and head); the mucus membranes of the oral cavity and lips (9%) and other sites (1%; stomach, small intestine, genital system and spleen)[2]. Tumors occur frequently in, at or near areas of chronic immune stimulation.

Oral EMPs appear to behave similarly to cutaneous EMPs—i.e. usually have a benign course with no related clinical signs. In contrast, dogs with colorectal EMPs often present with hematochezia, tenesmus, and rectal prolapse.

Amyloid deposition (primary, lambda light chains) is reported to be rare with colorectal EMPs.[2,3,4] When observed it occurs as small islands surrounded by tumor cells or as large sheets with occasional multinucleated giant cells. No correlation has been described for the presence of amyloid in plasmacytomas and

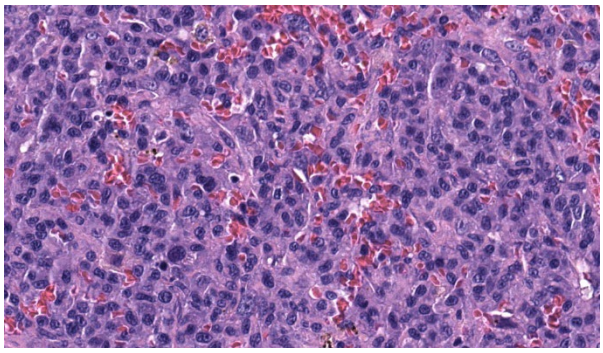

2-3. Colon, dog: Neoplastic round cells are moderately pleomorphic, with karyomegaly, nuclear indentation, and multinucleated forms. Neoplastic cells often have a perivascular clearing. (HE, 993x)

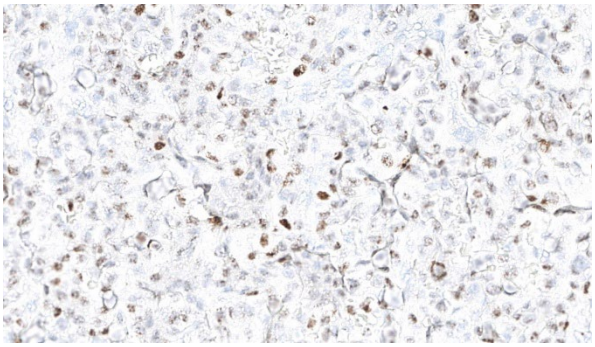

2-4. Colon, dog: Neoplastic cells demonstrate scattered moderate nuclear immunoreactivity for MUM1, a marker of plasma cells. (anti-MUM1, 890x)

the cell type, location, recurrence or biological behaviour.[1]

Dense cytoplasmic staining with methyl green pyronin stain (MGP) lends support to the diagnosis of an EMP but it is not specific for plasma cells and must be interpreted with caution.

The prognosis for colorectal plasmacytoma is generally good with complete excision. Recurrence follows incomplete surgical excision. Surgical excision was incomplete in this case and monitoring for possible local recurrence was encouraged.

Contributing Institution:
Prairie Diagnostic Services (PDS) and Department of Veterinary Pathology,
Western College of Veterinary Medicine,
https://wcvm.usask.ca/departments/vet-pathology.php

JPC Morphologic Diagnosis:
Colon: Plasmacytoma.

JPC Comment:
The contributor has provided a concise review of plasmacytomas, with a focus on those affecting the gastrointestinal tract. It bears restating, especially for trainees, that plasmacytomas are common submissions in a typical surgical pathology practice, with the skin, ear canal, and oral cavity as the most commonly seen locations. As with most Wednesday Slide Conference submissions, the workup in this case is excellent, with multiple additional stains, including immunomarkers, provided to demonstrate the appropriate histochemical behavior of these tumors. However, the vast majority of plasmacytomas are readily diagnosed on H&E section, based on the characteristic resemblance to traditional plasma cells, their often stereotypical location, and their characteristic arrangement in nests and packets. This is not shared by other round cell tumors, with the exception of transmissible venereal tumors.

One hallmark of a good surgical pathology report for neoplasia is an unimpeachable diagnosis based on all available information and special techniques; it should also provide, if available, information on the future behavior of the tumor in question. While prognostication for the individual animal should be avoided, published outcome data is always helpful for our clinical colleagues.

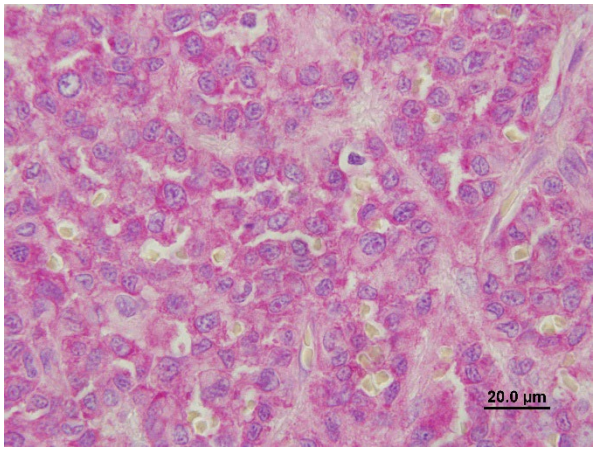

2-5. Colon, dog: The cytoplasm of neoplastic cells is strongly pyroninophilic. (Methyl green pyronin, 400x) (*Photo courtesy of*: Prairie Diagnostic Services (PDS) and Department of Veterinary Pathology, Western College of Veterinary Medicine, University of Saskatchewan.)

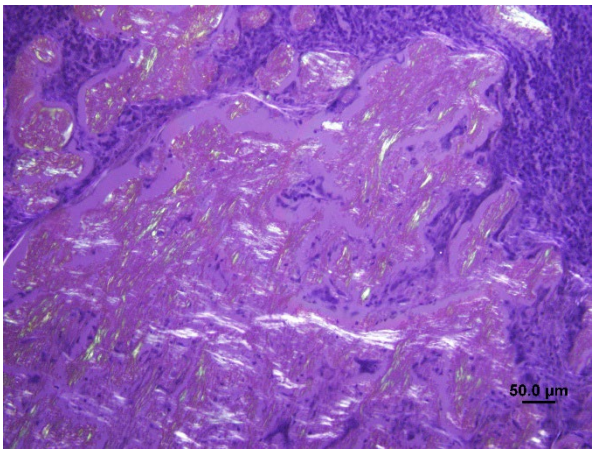

Colon, dog: Islands of amyloid exhibit apple-green birefringence when a Congo Red stain is viewed under polarized light. (Methyl green pyronin, 400x) (*Photo courtesy of*: Prairie Diagnostic Services (PDS) and Department of Veterinary Pathology, Western College of Veterinary Medicine, University of Saskatchewan.)

For oral plasmacytomas in dogs, Evenhuis *et al.* published an outstanding retrospective series of 45 cases in 2023.[5] In this study of 45 patients with oral plasmacytoma receiving a combination of surgery and adjunctive chemotherapy and radiation, the median survival time was 973 days. However, almost 33% of dogs in the study exhibited progression of plasma cell disease, with two cases evolving to myeloma.[5] Unfortunately, the authors did not find histologic criteria to predict which animals would develop progressive disease, although mitotic counts of less than three mitotic figures in a 2.37 mm² field were associated with a lack of tumor progression.[5] Moderate nuclear atypia, such as that seen in this particular case, was associated with progressive plasma cell disease, although it was not statistically significant.

A note on prognostication for the prudent surgical pathologist - In this study, the median survival time was 973 days, with survival ranging from 2 days to 4315 days. This illustrates the pitfalls of applying median survival times to any particular individual. These figures represent the center of a bell curve, and as pathologists, we cannot predict where in the spectrum a particular individual will fall. Using median survival times to attempt to predict the fate of any individual animal is fraught with peril. It may do great damage to one's reputation in the eyes of our clients.

Rannou *et al.* published an interesting case of a rectal plasmacytoma in a dog with numerous cytoplasmic hemosiderin granules within the cytoplasm of neoplastic plasma cells.[6] This is interesting, but this fairly uncommon finding has been reported fairly frequently in humans with plasmacytomas, with alcoholism as a comorbidity,

Finally, the contributors provide a relatively rarely used stain in their workup, the methyl green pyronin stain, which bears review for those unfamiliar with it. This stain employs two cationic dyes, methyl green and pyronin. Methyl green binds to phosphate radicals within DNA, staining it green. The pyronin Y component binds to negatively charged RNA, staining it red. In figure 2-5, the large amount of RNA responsible for the basophilia of plasma cell cytoplasm is pyroninophilic and stains red. (This stain is also excellent for staining Nissl substance in neurons and for demonstrating nucleoli in a wide range of cells.)

References:

1. Cangul IT, Wijnen M, van Garderen E and van den Ingh TSGAM. Clinicopathological aspects of canine cutaneous and mucocutaneous plasmacytomas. J Vet Med A, 2002; 49: 307-312.
2. Kupanoff PA, Popovitch CA, and Goldschmidt MH. Colorectal plasmacytomas; a

retrospective study of nine dogs. J Am Anim Hosp Assoc, 2006; 42: 3-43.

3. Ramos-Vara JA, Miller MA, Pace LW, Linke RP, Common RS and Watson GL. Intestinal multinodular Aλ-Amyloid deposition associated with extramedullary plasmacytoma in three dogs: clinipathological and immunohistochemical studies. J. Com Path, 1998; 119: 239-249
4. Ramos-Vara JA, Takahashi M, Ishihara T,Miller MA, Pace LW, Craft, D, Common R and Watson GL. Intestinal extramedullary plasmacytoma associated with amyloid deposition in three dogs: an ultrastructural and immunoelectron microscopic study. Ultrastruct Pathol, 1998; 22:393-4005.
5. Evenhuis JV, Oates A, Hoyer N, Vilander AC, Thamm DH, Worley DR. A retrospective study of canine oral extramedullary plasmacytoma over a 15-year period (July 2004-July 2019): Treatment, histologic parameters and clinical outcomes. Vet Comp Oncol. 2023 Jun;21(2):302-314.
6. Rannou B, Hélie P, Bédard C. Rectal plasmacytoma with intracellular hemosiderin in a dog. Vet Pathol. 2009 Nov;46(6):1181-4. doi: 10.1354/vp.08-VP-0266-R-CR. Epub 2009 Jul 15. PMID: 19605892.
7. Suvarna, S.K., Layton, C. and Bancroft, J.D. 2013, *Bancroft's Theory and Practice of Histological Techniques*, 7th ed, Churchill Livingstone Elsevier.

CASE III:

Signalment:
Cat (Felis catus), breed: European shorthair

10 years of age

Male (castrated)

History:
Anorexia and losing weight since two months. Some teeth were extracted. In the following days the cat developed corneal edema in the right eye. Clinic diagnosed a glaucoma. CT was performed to identify cause of glaucoma and check for dental problems. During induction the cat developed high heartrate. Thoracic imaging shows bilateral pneumothorax with aberrant lung tissue. Due to poor prognosis the cat was euthanized.

Gross Pathology:
The right eye is very firm compared to the left eye. The right eye has a red, diffusely opaque cornea. The lungs contain bilaterally, multifocal, white, shiny, firm, round noduli. Both kidneys contain multiple white, shiny, firm, expansile noduli in the cortices.

Laboratory Results:
None.

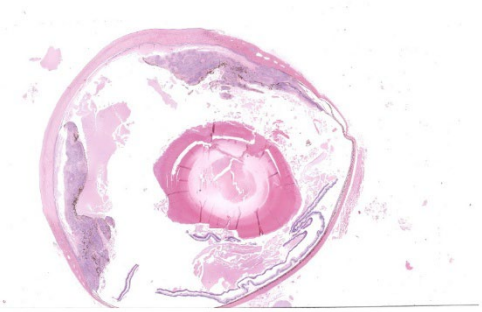

3-1. Eye, cat. A section of eye is submitted for examination.The iris and ciliary body is markedly expanded by a neoplasm which extends along the posterior aspect of the cornea, and along the surface of the retina. (HE, 9x)

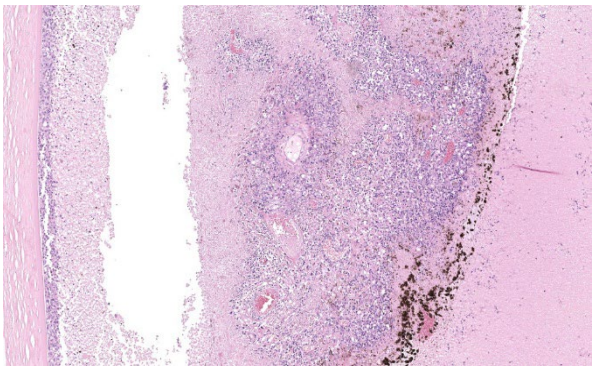

3-2. Eye, cat. The neoplasm expands the iris and coats the posterior aspect of the cornea. Within the iridal neoplasm, there are extensive areas of necrosis and foci of peritheliomatous survival. The anterior segment is filled with a pink proteinaceous fluid. (HE, 91x)

Microscopic Description:
Right eye: The iris is almost diffusely irregularly thickened with nodular protrusions in the vitreous. This thickening is due to a development of neoplastic cells that appear in the ciliary body and infiltrate the filtration angle. The neoplastic mass is moderately cellular, poorly demarcated, growing infiltratively and not encapsulated. The cells lie in contiguous fields, regularly surrounding a newly created vascular structure, supported by a varying amount of fibrovascular stroma. Cells are polygonic, varying in size but averaging about 10 µm in diameter, with poorly visible cell borders, abundant eosinophilic, fibrillar cytoplasm and a high nucleus:cytoplasm ratio. Some cells contain a compact dark brown to fine granular brown pigment. The nucleus is round, oval, to elongated, centrally located with finely stippled chromatin, and 1 to 3 eosinophilic nucleoli. There are sometimes cells with multiple nuclei, there is significant anisokaryosis and anisocytosis, including karyomegaly. Mitoses are 1 to 3 per 400x HPF. Multifocally there are large areas of eosinophilic amorphous material, bordered by neutrophilic granulocytes, cells with karyorrhexis and cell debris (necrosis). The sclera contains a vascular structure with a tumor embolism. The cornea contains multifocal formation of vascular structures (neovascularization) surrounded by some neutrophilic granulocytes. Some vascular structures in the sclera are bordered by many lymphocytes and plasma cells (lymph aggregates). Around the corpus ciliary there are many macrophages with brown pigment granules (melanomacrophages).

The lens multifocally contains many "bladder cells" (cataract). There is a detached lens apsule, but no reaction (cutting artefact). In the optic nerve some dilated myelin sheaths with foamy macrophages are present (digestion chambers, indicating degeneration).

Other organs (not submitted): similar neoplastic cells in the lung and kidney.

Contributor's Morphologic Diagnoses:
Right eye: ocular amelanotic melanoma; mild perivascular neutrophilic keratitis; cataract of the lens; multifocal, mild axonal degeneration of the optic nerve.

Contributor's Comment:
Almost all intraocular melanocytic tumors in cats represent a specific histologic and behavioral entity known as diffuse iris melanoma.[7] Moreover, Feline diffuse iris melanoma (FDIM) is by far the most common form of ocular melanocytic neoplasia.[5]

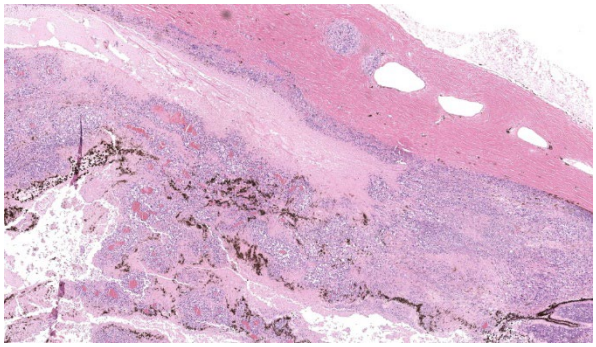

3-3. Eye, cat. The neoplasm expands the ciliary body, effaces the drainage angle, and infiltrates the sclera along the perivascular space. (HE, 54x)

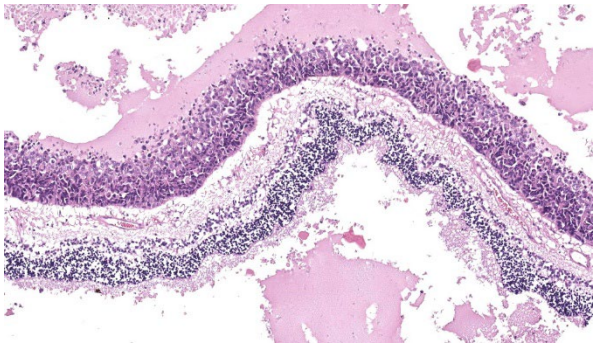

3-4. Eye, cat. The neoplasm also forms a mat along the inner surface of the artificially detached retina. There is moderate atrophy of the ganglion cell and inner nuclear and plexiform layers of the retina. (HE, 205x)

A wide variety in morphology is displayed including round or polygonal cell, spindle cell, balloon cell, anaplastic variants and giant cell types. The occurrence of amelanotic variants is low and can be clinically mistaken for inflammatory lesions.[5] "FDIM progressively expands through the iris, iridocorneal drainage angle and ciliary body, eventually penetrating the sclera".[5] Due to the neoplasm infiltrating the iridocorneal angle dyscoria, reduced pupil motility, thickening of the iris and secondary glaucoma may be observed.[5] Exfoliation of tumor cells into the anterior chamber and dissemination via the aqueous humor can result in metastasis as well as hematogenous spread via the intraocular vasculature.[3] The lung and liver are considered the most common sites of metastasis although metastases in the spleen, bones and regional lymph nodes have been reported.[6]

Extent of the tumor has a significant impact on survival times, invasion of neoplastic melanocytes into the ciliary body and animals with secondary glaucoma have reported lower survival rates compared to those without.[4]

Due to the wide variety of morphologic and pigmentation characteristics, a definitive diagnosis based on H&E alone is difficult. Additional immunohistochemical stains used for diagnostics of melanocytic neoplasia's include Melan-A, HMSA-5, S-100 and tyrosinase.[2,5]

Contributing Institution:
Veterinair Pathologisch Diagnostisch centrum – University of Utrecht
https://www.uu.nl/onderzoek/veterinair-pathologisch-diagnostisch-centrum/informatie-voor-dierenartsensen - Veterinair Pathologisch Diagnostisch Centrum - Universiteit Utrecht (uu.nl)

JPC Diagnoses:

1. Eye: Metastatic carcinoma.
2. Eye, lens: Cataract.

JPC Comment:
The contributor has provided an outstanding specimen of a pleomorphic, largely undifferentiated neoplasm in the feline globe. While melanoma must always be considered in the feline eye, it is not the only possibility, as post-traumatic ocular sarcomas may differentiate along a wide variety of morphologies. The feline uvea may also be a site of metastasis for poorly differentiated carcinomas.

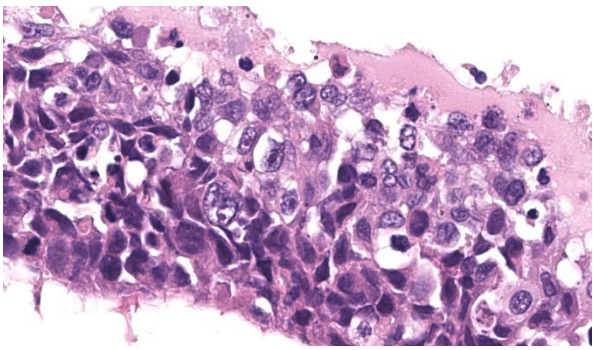

3-5. Neoplastic cells demonstrate marked pleomorphism. (HE, 1334x)

This thorny issue was addressed by Gran *et al.* in 2016[2] in their retrospective review of 75 neoplasms of the feline globe. In this excellent review, immunohistochemical labeling of eight of the 75 cases ultimately conflicted with the initial morphologic diagnosis rendered on the H&E section. Discordant diagnoses included four tumors which were initially diagnosed as lymphoma and four as ocular sarcoma.[2] Immunohistochemical testing amended the diagnosis of three of the lymphomas to melanoma, and the final case to ciliary body adenocarcinoma[2]. Two of the cases originally diagnosed as sarcoma ultimately demonstrated an immunohistochemical profile for melanoma, one for metastatic carcinoma, and the final case remained undifferentiated.[2]

In this case, the diagnosis of melanoma, particularly amelanotic melanoma, in the absence of any additional histochemical or immunohistochemical staining is somewhat problematic, especially in light of the findings of Grahn *et al.* discussed above.

To confirm the contributor's diagnosis of amelanotic melanoma, additional stains were run at the Joint Pathology Center, including Fontana-Masson, tyrosinase, MelanA, PNL2, and S-100. Neoplastic cells were immunonegative for all of these markers. Neoplastic cells demonstrate strong cytoplasmic immunopositivity for cytokeratin and approximately 10% of the neoplastic cells also demonstrate moderate immunoreactivity for vimentin.

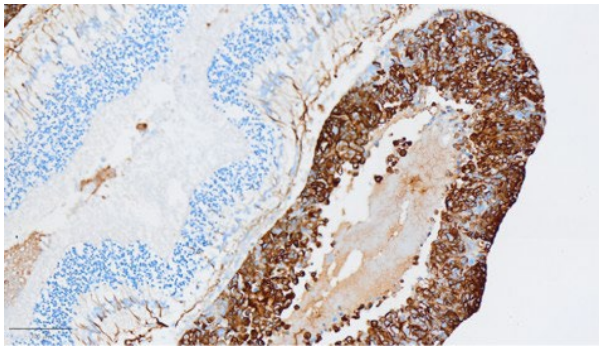

3-6. Eye, cat. Neoplastic cells demonstrate strong cytoplasmic immunoreactivity for cytokeratin, confirming a diagnosis of metastatic carcinoma. (anti – AE1/AE3, 1330x)

Based on the strong immunopositivity for cytokeratin, a diagnosis of metastatic carcinoma was made in this case. An additional histologic finding which supports this finding is the "carpeting" of the inside of the eye by the neoplastic cells, which has been identified as a histologic feature of carcinomas metastatic to the eye in the dog and cat [1,8], and in a previous WSC case of feline pulmonary carcinoma metastatic to the eye (WSC 2014-2014 Conference 24, Case 1).

The JPC morphologic diagnosis is a simple one and to the eyes of some, may not reflect all of the histologic changes that may be found in this eye. However, in traditional JPC (and AFIP before it) fashion, the morphologic diagnosis of a neoplasm reflect the tumor, and not all of the secondary changes that appear over time because of it. We did not consider the cataract secondary to the tumor in this case, so we provided a second morphologic diagnosis for a second, likely independent pathologic process.

References:

1. Dubielzig RR, Ketring KL, McLellan GJ. Veterinary Ocular Pathology: a comparative review. 2010.
2. Grahn BH, Peiffer RL, Cullen CL. Classification of feline intraocular neoplasms based on morphology, histochemical staining, and immunohistochemical labeling. *Vet Ophthalmol*. 2016: 9(6), 395-403.

3. Jajou S. Uveal amelanotic melanoma in a ragdoll cat. *Can Vet J*. 2020: Jun 61(6):645-647.
4. Kalishman JB, Chappell R, Flood LA. A matched observational study of survival in cats with enucleation due to diffuse iris melanoma. *Vet Ophthalmol*. 1998 1(1), 25-29.
5. Kayes D & Blacklock B. Feline Uveal Melanoma Review: Our Current Understanding and Recent Research Advances. *Vet Sciences*. 2022: 9(2), 46.
6. Patnaik AK & Mooney S. Feline melanoma: a comparative study of ocular, oral, and dermal neoplasms. *Vet Path*. 1988: 25(2), 105-112.
7. Wilcock BP, Bradley Njaa L. Special senses. In: *Jubb, Kennedy, and Palmer's Pathology of Domestic Animals*. Sixth ed., vol 1, Philadelphia, PA: Elsevier Saunders; 2016: 407
8. Stocklein H, Taylor RP, Shaw GC, Clarke LL. Histomorphologic and immunohistochemical characteristics of intraocular metastatic carcinomas of presumed pulmonary origin in cats: A retrospective case series from 2019 to 2025. *Veterinary Pathology*. 2026;63(5):820-824. doi:10.1177/03009858261445996

CASE IV:

Signalment:
128-week-old male C57BL6/N wild type mouse (Mus musculus).

History:
Found dead in the cage. Animal received a standard chow diet equals to 10% reduction of normal calorie intake. This animal developed a distended abdomen, food intake gradually decreased, while body weight was increasing.

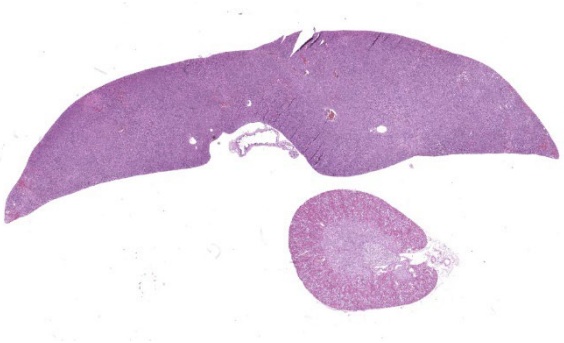

4-1. Liver, kidney, mouse: At subgross magnification, multiple small foci of necrosis are visible, scattered throughout the liver parenchyma. The proximal convoluted tubules in the kidney are hypereosinophilic. (HE,15x)

Gross Pathology:
The liver was moderately enlarged, with rounded edges, beige to red in color and with an irregular bosselated surface.

The spleen was moderately enlarged, with multifocal to coalescing beige nodules.

Laboratory Results:
Not applicable.

Microscopic Description:
Liver: The normal hepatic architecture is markedly distorted and obscured by a multifocal to coalescing, highly infiltrative, poorly demarcated, unencapsulated, and densely cellular neoplasm. Neoplastic cells are arranged in sheets and small aggregates, infiltrating and expanding hepatic sinusoids and frequently displacing or replacing hepatocyte cords and stroma, thereby effacing normal lobular organization. The neoplastic cells are pleomorphic, with variably distinct cell borders, a moderate nuclear-to-cytoplasmic ratio, and a moderate amount of finely granular eosinophilic cytoplasm. Nuclei are round to ovoid with clumped chromatin and occasional prominent nucleoli. Multinucleated neoplastic cells are occasionally observed. There is marked

anisocytosis and anisokaryosis. Mitotic figures are rare (1 in 10 high-power fields; 2.37 mm^2). Neoplastic cells multifocally infiltrate the walls of larger vessels and frequently extend into the vascular lumina, forming intravascular aggregates (neoplastic emboli). Adjacent hepatocytes are frequently shrunken (atrophic), and surrounding sinusoids are either expanded by neoplastic cells or engorged with erythrocytes. Multifocal areas characterized by replacement of tissue with amorphous eosinophilic material and karyorrhectic debris (lytic necrosis) are also present, often associated with extravasated erythrocytes (hemorrhages) and occasional hemosiderin-laden macrophages. Scattered within hepatic sinusoids are small aggregates of small round cells with hyperchromatic nuclei, granulocytes and occasional megakaryocytes (extramedullary hematopoiesis).

Kidney: The tubular epithelial cells of the proximal tubules are diffusely distended by numerous intensely eosinophilic, variably sized cytoplasmic granules (hyaline droplets). Occasional tubular epithelial cells contain fine intracytoplasmic brown pigment (presumed lipofuscin or hemosiderin). Rarely, tubular lumina contain homogeneous eosinophilic material (protein casts).

Additional Findings (not present on the submitted slide): The neoplasm also extensively involved the spleen. Immunohistochemical staining for Iba1 also demonstrated intravascular aggregates of pleomorphic positive cells (neoplastic emboli) within vessels of the kidneys and lungs. Additionally, a fibrin thrombus was observed within the right ventricular chamber of the heart, adhering to the free wall and the septum.

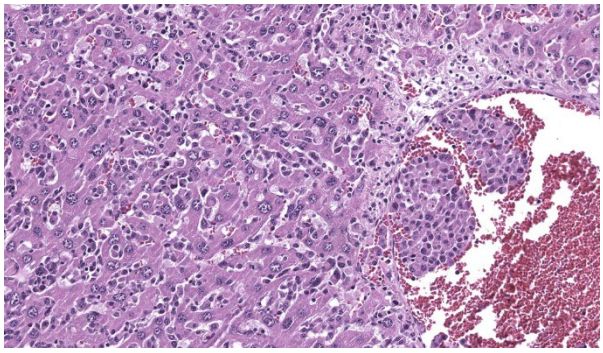

4-2. Liver, mouse: sinusoids are filled and expanded, and the wall of a hepatic vein is traversed by neoplastic histiocytes. (HE, 381x).

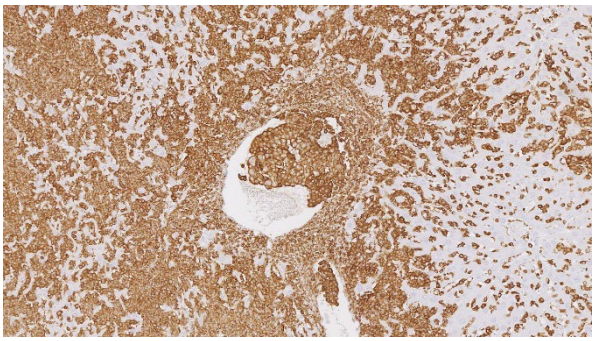

4-3. Liver, mouse: Neoplastic round cells demonstrate strong cytoplasmic immunoreactivity for IBA-1. (anti-IBA-1, 100x) (*Photo courtesy of*: Laboratory for Animal Model Pathology, Institute of Veterinary Pathology, University of Zurich, https://www.vetpathology.uzh.ch/de/Andere-Services/lamp.html.)

staining for Iba1 also demonstrated intravascular aggregates of pleomorphic positive cells (neoplastic emboli) within vessels of the kidneys and lungs. Additionally, a fibrin thrombus was observed within the right ventricular chamber of the heart, adhering to the free wall and the septum.

Immunohistochemistry reveals strong and diffuse cytoplasmic expression of Iba1 in the neoplastic cells. Lysozyme expression is evident in occasional neoplastic cells.
Immunohistochemistry reveals that the granules are diffusely positive for lysozyme. Occasional intravascular Iba1 positive cells are also evident.

Additional Findings (not present on the submitted slide): The neoplasm also extensively involved the spleen. Immunohistochemical staining for Iba1 also demonstrated intravascular aggregates of pleomorphic positive cells (neoplastic emboli) within vessels of the kidneys and lungs. Additionally, a fibrin thrombus was observed within the right ventricular chamber of the heart, adhering to the free wall and the septum.

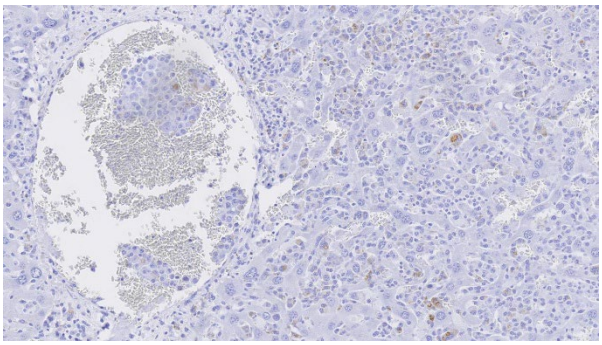

4-4. Liver, mouse: Occasional neoplastic cells exhibit granular cytoplasmic positivity for lysozyme (anti-lysozyme-1, 100x) (*Photo courtesy of*: Laboratory for Animal Model Pathology, Institute of Veterinary Pathology, University of Zurich, https://www.vetpathology.uzh.ch/de/Andere-Services/lamp.html.)

Contributor's Morphologic Diagnoses:
Liver: histiocytic sarcoma with vascular wall invasion and neoplastic emboli.

Kidney: hyaline droplet accumulation in the tubular epithelial cells and rare protein casts.

Contributor's Comment:
Histiocytic sarcoma in mice is a relatively frequent and well-characterized hematopoietic neoplasm arising from the mononuclear phagocyte system, typically involving organs rich in resident macrophages, including the liver and spleen.[2,6] In this case, the presence of multifocal to coalescing infiltrates of pleomorphic histiocytic cells in the liver, their intravascular localization, and strong immunolabeling with the histiocytic marker Iba1 are consistent with a diagnosis of histiocytic sarcoma.[6]

An associated and noteworthy finding in this case is the presence of numerous eosinophilic hyaline droplets in the proximal tubular epithelial cells of the kidneys. These droplets are considered a secondary, paraneoplastic change related to histiocytic sarcoma, due to the systemic overproduction of lysozyme - a major secretory product of neoplastic histiocytes.[4,8]

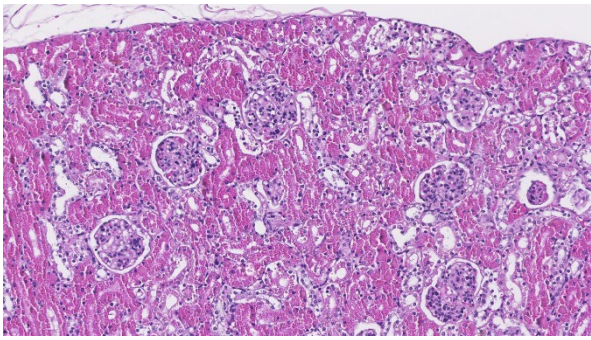

4-5. Kidney, mouse: The tubular epithelial cells of the proximal tubules are diffusely distended by numerous intensely eosinophilic, variably sized cytoplasmic granules (HE, 200X) (*Photo courtesy of*: Laboratory for Animal Model Pathology, Institute of Veterinary Pathology, University of Zurich, https://www.vetpathology.uzh.ch/de/Andere-Services/lamp.html.)

Hard and Snowden demonstrated that lysozyme-rich hyaline droplets are present in approximately 96% of rats and 55% of mice with histiocytic sarcoma, often correlating with tumor burden and distribution.[4] Immunohistochemistry confirmed that these droplets were strongly positive for lysozyme (muramidase) and negative for α_1-antitrypsin, immunoglobulin, albumin, and α_2u-globulin.[4] Luz and Murray further supported these findings across multiple mouse strains and emphasized that the visualization of hyaline droplets can be dependent on the eosin formulation used during staining, with alcoholic eosin providing superior contrast[8].

From a mechanistic standpoint, overproduction of lysozyme by the neoplastic macrophages overwhelms the normal tubular degradation capacity. Lysozyme is a small (≈14 kDa) basic protein which is freely filtered and normally reabsorbed and catabolized in lysosomes of the tubular epithelial cells of the

proximal renal tubule.[4,9,10] Microscopically these appear as abundant, eosinophilic, homogenous cytoplasmic droplets (best seen in the P2 segment of proximal tubules).[4]
This parallels human monocytic leukemias where neoplastic cells produce lysozyme that similarly induce accumulation of protein droplets in the proximal tubule.[9]

The detection of these renal hyaline droplets should prompt careful evaluation for underlying histiocytic neoplasia in rodents, even in the absence of clinical suspicion. From a toxicologic pathology perspective, it is important to distinguish tumor-induced hyaline droplet accumulation from chemically-induced nephropathy, particularly in regulatory studies, to avoid misinterpretation of compound-related effects.[2,4] Hyaline droplet accumulation in the tubular epithelial cells represents an important differential feature to distinguish this lesion from α2u-globulin nephropathy, which occurs only in male rats and is chemically induced.[2,4] Certain chemicals (e.g. hydrocarbons) bind α2u-globulin and prevent its lysosomal degradation, so the protein accumulates in tubular lysosomes as spherical or crystalloid "hyaline droplets".[3,4,11] These droplets are strongly indicative of male rat α2u-globulin nephropathy: they are strongly positive for α2u-globulin and absent in normal female rats or in mice (mice lack α2u-globulin).[4,7]

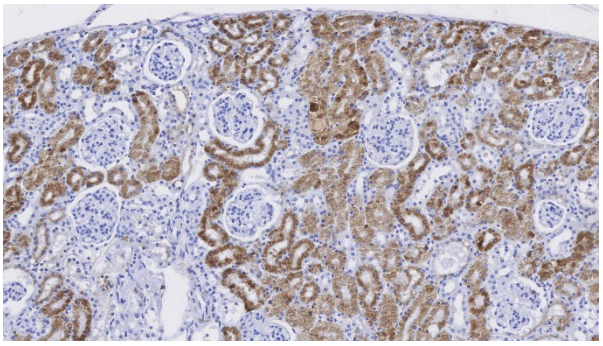

4-6. Kidney, mouse: The hyaline droplets are diffusely immunopositive for lysozyme (anti-lysozyme-1, 200X) (*Photo courtesy of*: Laboratory for Animal Model Pathology, Institute of Veterinary Pathology, University of Zurich, https://www.vetpathology.uzh.ch/de/Andere-Services/lamp.html.)

Other neoplastic or degenerative causes of hyaline droplet accumulation in renal tubular epithelial cells are far less common but have been reported. Certain lymphomas or leukemias in mice have been associated with renal hyaline droplets.[1] For example, Decker *et al.* described hyaline droplets in CD-1 mice with lymphoma.[1] Mononuclear cell (large granular lymphocyte) leukemias in Fischer rats can have scattered pigmented granules in tubules (iron or lipofuscin, not lysozyme).[4,5] In both the mouse and rat, any chronic severe proteinuric condition (e.g. glomerular disease or advanced chronic progressive nephropathy) can produce hyaline inclusions, but again the protein composition differs.[2]

Contributing Institution:
Laboratory for Animal Model Pathology
Institute of Veterinary Pathology
University of Zurich
Zurich, Switzerland
https://www.vetpathology.uzh.ch/de/Andere-Services/lamp.html

JPC Diagnosis:
1. Liver: Histiocytic sarcoma.

2. Kidney, proximal convoluted tubules: Hyaline droplet accumulation.

JPC Comment:
The contributor has provided an excellent review of the significance of hyaline droplet disease and its positive correlation with the presence of histiocytic sarcoma in affected individuals.

For a somewhat wider ranging review of this tumor (and specifically in C57Bl6 mice, the strain of the submitted individual in this case), the reader is referred to an excellent publication by Janke et al (2026).[6] While a rare tumor in humans, this tumor is much more common

in mice, including the C57Bl6 strain, where in various studies it ranges from 2-34.7%.[6] It is a tumor of many different morphologies, which has resulted in its publication as a wide range of tumors, including lymphoma, Schwannoma, endometrial sarcoma (spindle cells is a morphologic hallmark of this tumor) and often many others.[6]

Histiocytic sarcoma in mice is renowned for morphologic heterogeneity; however, round cells and spindle cells are typically present in the same tumor. In the review by Janke, 39% of tumors demonstrated a range of cellular pleomorphism, and multinucleated cells were seen in 21% of cases. Intravascular involvement, as seen in this case, was present in 61% of tumors in that study and areas of necrosis was present in 42%.

Additionally, to further complicate the diagnostic picture (at least on HE review), this tumor often coexists (and may be commingled) with murine lymphoma or leukemia (12% of the animals in the Janke study).[6] B-cell tumors predominated at a rate of 88%.[6]

Extramedullary hematopoiesis is a common finding in this tumor, both within the tumor and in other organs which may lack tumor cells (typically in affected animals, the spleen is rife with EMH, but rarely the tumor itself). In the Janke study, EMH was seen in 75% of tumors.[6] Splenic hematopoiesis was first reported by Frith et al n 1990[12], and hepatic hematopoiesis was reported three years later by Lacroix-Triki *et al*.[12] While the definitive connection between histiocytic sarcoma and extramedullary hematopoeisis (both within the tumor itself and in remote locations) remains elusive, macrophages are well known for their vital roles in erythropoiesis, which include support of hematopoetic stem cells as well as the removal of senescent stem cells, and creating and regulating a specialized microenvironment for both erythroid and megakaryocyte precursors.[14]

References:

1. Decker JH, Dochterman LW, Niquette AL, Brej M. Association of Renal Tubular Hyaline Droplets with Lymphoma in CD-1 Mice. *Toxicol Pathol*. 2012;40(4):651–655.
2. Frazier KS, Seely JC, Hard GC, *et al.* Proliferative and Nonproliferative Lesions of the Rat and Mouse Urinary System. *Toxicol Pathol.* 2012;40(4_suppl):14S-86S.
3. Hamamura M, Oshikata T, Katoku K, Tsuchitani M, Yamaguchi R. Two types of deposits, hyaline droplets and eosinophilic bodies, associated with α2u-globulin accumulation in the rat kidney. *J Toxicol Pathol*. 2017;30(4):275–282.
4. Hard GC, Snowden RT. Hyaline Droplet Accumulation in Rodent Kidney Proximal Tubules: An Association with Histiocytic Sarcoma. *Toxicol Pathol.* 1991;19(2):88–97.
5. Ishmael J, Dugard PH. A review of perchloroethylene and rat mononuclear cell leukemia. 2006;45(2):178–184.
6. Janke LJ, Rehg JE. The many faces of mouse histiocytic sarcoma in C57BL/6J mice. *Vet Pathol*. 2023;60(4):443–460.
7. Lehman-McKeeman LD, Caudill D. Biochemical basis for mouse resistance to hyaline droplet nephropathy: Lack of relevance of the α2u-globulin protein superfamily in this male rat-specific syndrome. *Toxicol Appl Pharmacol*. 1992;112(2):214–221.
8. Luz A, Murray AB. Hyaline Droplet Accumulation in Kidney Proximal Tubules of Mice with Histiocytic Sarcoma. *Toxicol Pathol*. 1991;19(4–2):670–671.

9. Santoriello D, Andal LM, Cox R, D'Agati VD, Markowitz GS. Lysozyme-Induced Nephropathy. *Kidney Int Rep*. 2017;2(1):84–88.
10. Singh G, Katyal SL, Brown WE, Collins DL, Mason RJ. Pulmonary Lysozyme-A Secretory Protein of Type II Pneumocytes in the Rat. 1988;138(5):1261–1267.
11. Urinary System Kidney, Renal Tubule - Accumulation, Hyaline Droplet, https://ntp.niehs.nih.gov/atlas/nnl/urinary-system/kidney/RenalTubule-AccumulationHyalineDroplet. *Nonneoplastic Lesion Atlas - National Toxicology Program*.
12. Frith CH (1990). Histiocytic sarcoma, mouse. In: *Monographs on Pathology of Laboratory Animals*. *Hemopoietic system*, Jones TC,Ward JM, Mohr U, Hunt RD (eds). Springer-Verlag, Berlin, Heidelberg, pp 58–65.
13. Lacroix-Triki M, Lacoste-Collin L, Jozan S, Charlet JP, Caratero C, Courtade M. Histiocytic sarcoma in C57BL/6J female mice is associated with liver hematopoiesis: review of 41 cases. Toxicol Pathol. 2003 31(3):304-9.
14. Huang H, Gao M, Vinchi F, An X, Li W, Wang Y. Macrophages in Hematopoiesis and Related Blood Diseases. Genomics Proteomics Bioinformatics. 2025 23(6):qzaf112. doi: 10.1093/gpbjnl/qzaf112.